Original Article

Value of cardiac magnetic resonance feature tracking technology in the differential diagnosis of isolated left ventricular noncompaction and dilated cardiomyopathy

Lina Zhu, Jiang Wu, Xiaoyong Hao, Xuan Li

Department of Magnetic Resonance, Shanxi Cardiovascular Hospital, Taiyuan, China

Contributions: (I) Conception and design: L Zhu, J Wu; (II) Administrative support: J Wu; (III) Provision of study materials or patients: J Wu; (IV) Collection and assembly of data: L Zhu, X Hao, X Li; (V) Data analysis and interpretation: L Zhu, J Wu, X Hao; (VI) Manuscript writing: All authors; (VII) Final approval of manuscript: All authors.

Correspondence to: Jiang Wu. Department of Magnetic Resonance, Shanxi Cardiovascular Hospital, No. 18 Yifen Street, Wanbolin District, Taiyuan, China. Email: wujiang1024@sina.com.

Background: This study explored the value of myocardial strain in the differential diagnosis of isolated left ventricular myocardial noncompaction (ILVNC) and dilated cardiomyopathy (DCM) using cardiac magnetic resonance (CMR) feature tracking technology.

Methods: This retrospective analysis was performed on consecutive patients (25 with ILVNC, 30 with DCM, and 30 healthy controls) presenting to Shanxi Cardiovascular Hospital. All ILVNC patients met echocardiographic and CMR criteria for ventricular non-compaction. All patients with DCM met the 2016 American Heart Association and 2018 Chinese Medical Association Cardiovascular Branch diagnostic criteria. cvi42 software (Circle Cardiovascular Imaging) was used to measure radial, circumferential, and longitudinal strain (LS) globally and in segments of the left ventricle. Analysis of variance was used to compare strains among groups and among different segments within the same group. Receiver operating characteristic (ROC) curves were used to evaluate the diagnostic efficacy of different parameters in ILVNC and DCM.

Results: Basal circumferential strain was lower in the DCM than in the ILVNC group (P=0.05). Both median and apical LS were lower in the ILVNC than in DCM group (P=0.02 and P=0.01, respectively). ROC curves showed that apical LS was the most effective in distinguishing ILVNC from DCM [area under the curve (AUC) =0.883; P<0.001; 95% CI: 0.850–0.977]. Comparing strains among different segments within the same group revealed that in DCM, the circumferential and LS of the apex were higher than those of the basal segment, which is consistent with the pattern in healthy controls; however, has no such regular pattern was seen in ILVNC.

Conclusions: Myocardial strain parameters are of considerable value in the differential diagnosis of ILVNC and DCM. Differences in patterns between ILVNC and DCM can be sensitively identified, providing more comprehensive information for early clinical diagnosis.

Keywords: Cardiac magnetic resonance feature tracking technology; dilated cardiomyopathy (DCM); isolated left ventricular myocardial noncompaction (ILVNC); strain

Submitted Jul 05, 2022. Accepted for publication Dec 21, 2022. Published online Feb 06, 2023.
doi: 10.21037/qims-22-710
View this article at: https://dx.doi.org/10.21037/qims-22-710

Introduction

Isolated left ventricular myocardial noncompaction (ILVNC) is a rare cardiomyopathy characterized by a massive trabecular protrusion under the left ventricular (LV) endocardium, with the trabeculae connected to the LV lumen, and no other cardiac congenital malformations (1). Dilated cardiomyopathy (DCM) is a type of cardiomyopathy characterized by LV enlargement with systolic dysfunction. Almost all patients with advanced DCM exhibit varying degrees of increased trabeculae in the LV lumen and partially meet the diagnostic imaging criteria for ILVNC (2). At present, diagnoses of ILVNC are primarily based on imaging examinations and clinical history. The clinical manifestations of ILVNC in patients vary from asymptomatic to progressive heart failure. Imaging diagnosis primarily relies on echocardiography and cardiac magnetic resonance imaging (MRI) measurement of the ratio of LV end-diastolic noncompacted (NC) to compacted (C) myocardium, but cut-off values remain to be determined (3). Due to the similarities in clinical and imaging manifestations between ILVNC and DCM, it is sometimes difficult to make a differential diagnosis. The triad of heart failure, thromboembolic events, and tachyarrhythmias makes ILVNC a hereditary cardiomyopathy with high mortality and morbidity. Therefore, early screening and diagnosis will benefit patients with milder symptoms, thereby improving overall prognosis (4).

Cardiac magnetic resonance feature tracking (CMR-FT) is a new technique developed in recent years to quantitatively analyze myocardial strain (5). CMR-FT can be used to measure the displacement of the target myocardium from different directions and to obtain global and segmental parameters of myocardial strain, including radial strain (RS), circumferential strain (CS), and longitudinal strain (LS); it can also be used to evaluate changes in cardiac function (6,7). In this study, we used CMR-FT to explore the value of myocardial strain in distinguishing ILVNC from DCM. We present the following article in accordance with the STARD reporting checklist (available at https://qims.amegroups.com/article/view/10.21037/qims-22-710/rc).

Methods

General information

This study was conducted in accordance with the Declaration of Helsinki (as revised in 2013) and was approved by the Medical Ethics Committee of Shanxi Cardiovascular Hospital. All participants provided written informed consent. Consecutive ILVNC and DCM patients who presented at Shanxi Cardiovascular Hospital between March 2017 and May 2021 and in whom diagnoses were confirmed by clinical and imaging were included in this study. Patients who underwent CMR in the hospital during the period and who did not have any abnormalities were used as the healthy control group.

Inclusion criteria for ILVNC

To be eligible for inclusion in the ILVNC group, patients had to meet the echocardiographic criteria of Jenni *et al.* (8), as well as the following CMR and clinical criteria: (I) 2 layers of the LV myocardium, namely a C and NC layer, involving at least the apex; (II) an end-diastolic NC to C ratio >2.3 (Petersen criterion) on long-axis views (9) and ≥3 on short-axis views (10); (III) an NC mass >20% of the global LV mass (Jacquier criterion) (11); (IV) no pathological (pressure/volume load; e.g., hypertension) or physiological (pregnancy or long-term strenuous exercise) remodeling factors leading to excessive trabeculation; and (V) an LV ejection fraction (LVEF) ≤45%.

Inclusion criteria for DCM

To be eligible for inclusion in the DCM group, patients had to meet the following diagnostic criteria set by the American Heart Association in 2016 (12) and the Chinese Medical Association Cardiovascular Branch in 2018 (13): (I) LV end-diastolic dimension >5.5 cm in men and >5.0 cm in women, or a standard deviation >2-fold the normal value; (II) reduced overall systolic function of the LV and LVEF <45% or fractional shortening (FS) <25%; and (III) at least 3 segments with excessive trabeculation (NC/C >1.0).

Inclusion criteria for the healthy control group

Patients without history of cardiovascular disease, with normal findings on chest radiography, electrocardiography, and echocardiography, and normal cardiac function on CMR were eligible for inclusion in the healthy control group.

Exclusion criteria

For all participants, the following exclusion criteria were applied: (I) concomitant coronary artery disease, other types of cardiomyopathy, valvular disease, or congenital heart

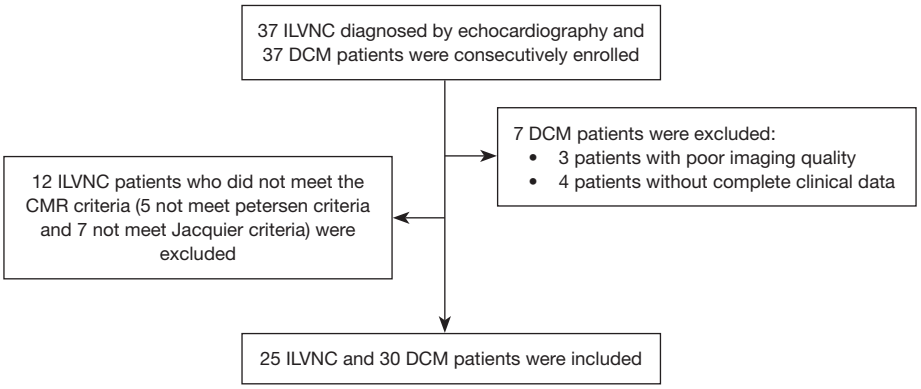

Figure 1 Flowchart showing population enrollment. CMR, cardiac magnetic resonance imaging; DCM, dilated cardiomyopathy; ILVNC, isolated left ventricular myocardial noncompaction.

disease; (II) contraindications for MRI examinations (e.g., implantation of cardioversion defibrillators or pacemakers incompatible with MRI, metal devices or foreign objects, and severe claustrophobia); and (III) image quality insufficient for accurate image postprocessing evaluation (*Figure 1*).

Data collection

Images were acquired on a 1.5-T MRI scanner (Signa HDxt; GE Healthcare, Chicago, IL, USA) equipped with an 8-channel phased-array cardiac receiver coil and electrocardiogram triggering and respiratory gating technology. Cines MRI with a fast imaging employing steady-state acquisition (FIESTA) sequence was performed in the conventional cardiac short- and long-axis planes (2-, 3-, and 4-chamber) at the end of expiration. Each cardiac cycle was divided into 20 phases for image reconstruction. The parameters were as follows: repetition time (TR) 3.0 ms, echo time (TE) 1.3 ms, field of view (FOV) 350 mm × 350 mm, matrix 192×224, and flip angle 55°. The short-axis sequence scanned approximately 7–9 layers from the basal segment to the apex depending on the fixed layer thickness and layer spacing. The parameters were the following: slice thickness 8 mm, slice spacing 2 mm, TR 3.5 ms, TE 1.5 ms, FOV 360 mm × 360 mm, matrix 192×224, flip angle 55°, and 20 phases per cardiac cycle. Each layer was scanned for 9–15 s.

Data postprocessing

Data were imported into cvi42 postprocessing software (version 5.11.3; Circle Cardiovascular Imaging, Calgary, AB, Canada). The LV short-axis images were imported into the Short 3D module, and the LV endocardium and epicardium were automatically delineated at the end of diastole and systole to generate cardiac function parameters, including LV end-diastolic volume, LV end-systolic volume, LV stroke volume, LVEF, and left ventricular cardiac output. If the outline was inconsistent with the actual boundary, the position of the outline was corrected manually.

Strain analysis was performed using the Tissue Tracking module. The LV short-axis, and 2- and 4-chamber cardiac cine images were imported into the module, and then the endocardium and epicardium were automatically delineated at the end of diastole and systole, with the LV and right ventricular cutoff points being marked. The myocardial strain parameters (global and LV segments) RS, CS, and LS were obtained through automatic postprocessing using cvi42 software (*Figure 2*).

In end-diastole, trabeculation was not included in the automatically delineated areas when measuring cardiac function or myocardial strain. All data were independently obtained by 3 radiologists (≥5 years' experience in CMR) in a double-blind manner (i.e., neither the radiologists nor the subjects had any information regarding the experimental process, and the radiologists did not have access to clinical

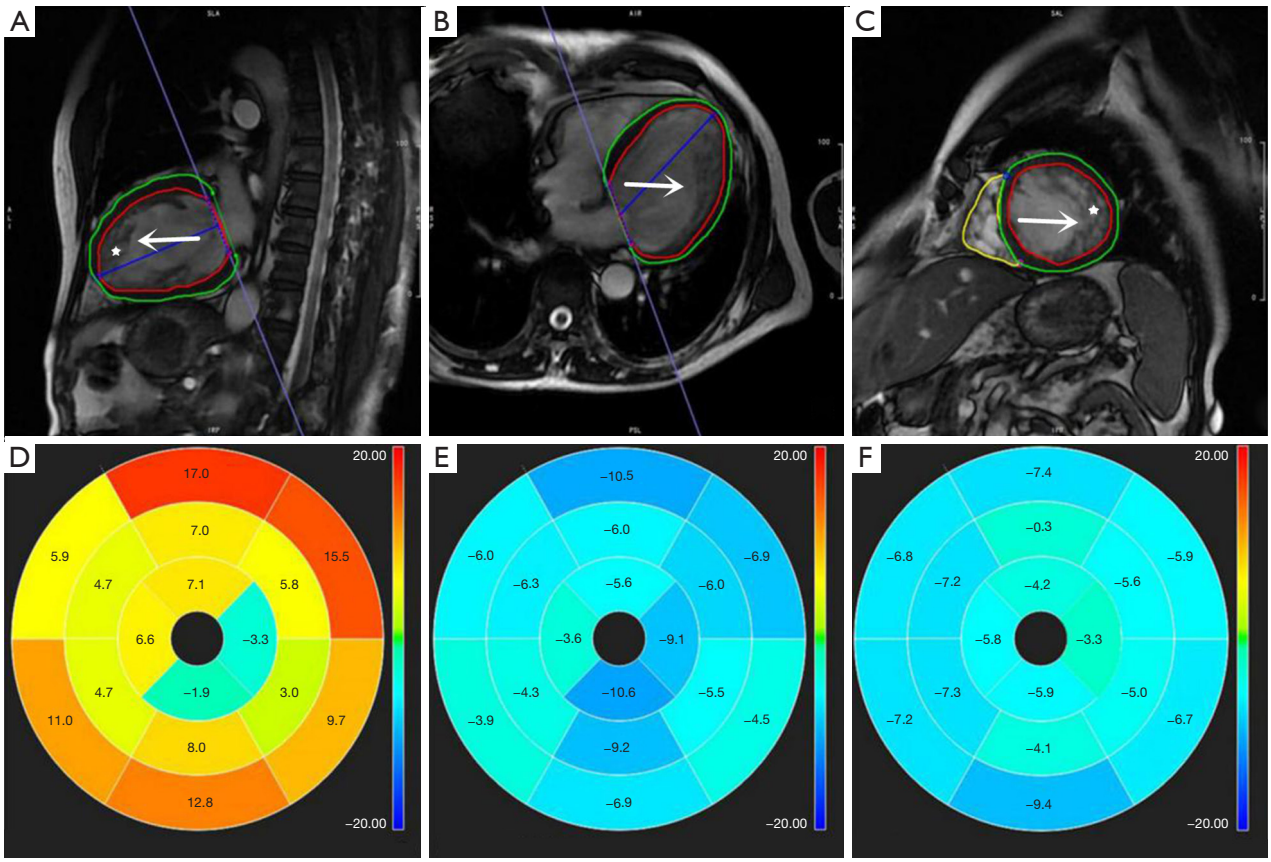

Figure 2 Postprocessing images of LV myocardial strain in a 66-year-old male with a history of ventricular tachycardia and ILVNC. A large number of loose trabeculae muscle bundles (white arrows) and deeply recessed crypts (white five-pointed stars) can be seen on the free wall and apex of the LV. (A-C) Outlines of the endocardium (red) and epicardium (green) boundaries in 2-chamber (A), 4-chamber (B), and short-axis (C) cine images; the LV and right ventricular demarcation points were defined in short-axis images (C; yellow). (D-F) Bull's-eye images of radial (D), circumferential (E), and longitudinal (F) strain in the 16 segments. LV, left ventricular; ILVNC, isolated LV myocardial noncompaction.

information). Data were averaged to obtain a final result. The measurement consistency of different observers was evaluated through intraclass correlation coefficients (ICCs). Due to the partial volume effect, the apical cap (segment 17) was excluded.

Statistical analysis

Data were analyzed using SPSS 19.0 (IBM Corp., Armonk, NY, USA). The normality of the data was tested using the Shapiro-Wilk test, and normally distributed continuous variables are presented as the mean ± SD. The homogeneity of variance was tested using the Levene test. Analysis of variance (ANOVA) was used to compare age, body mass index (BMI), the NC to C ratio, cardiac function, and strain between groups, as well as the strain between different segments within each of the 3 groups. If a significant difference was detected, a least significant difference (LSD) comparison was performed if there was a significant difference. Since gender belonged to a categorical variable, it was compared between groups using a chi-squared test. The diagnostic efficacy of different parameters in differentiating ILVNC from DCM was evaluated through receiver operating characteristic (ROC) curve analysis, and determination of the best cutoff value. Statistical significance was set at $P<0.05$.

Table 1 Baseline characteristics of the study population

Characteristics	ILVNC (n=25)	DCM (n=30)	CG (n=30)	P value
Age (years)	45.92±15.42	51.20±12.51	43.48±13.06	0.13
Male	12 (48.0)	16 (53.0)	13 (43.0)	0.54
BMI (kg/m^2)	23.62±2.58	22.68±3.19	22.96±2.14	0.25
NC/C ratio				
LAX	2.95±0.46	2.16±0.32	–	<0.001
SAX	3.53±0.28	2.36±0.25	–	<0.001
Clinical symptoms				
Chest tightness and shortness of breath	20 (80.0)	25 (83.0)	–	–
Palpitations	12 (48.0)	8 (27.0)	–	–
Syncope	3 (12.0)	5 (17.0)	–	–
Dyspnea	6 (24.0)	20 (67.0)	–	–
ECG examination				
Ventricular arrhythmia	13 (52.0)	10 (33.0)	–	–
Left bundle branch block	1 (4.0)	13 (43.0)	–	–
ST-T change	8 (32.0)	3 (10.0)	–	–
Atrial fibrillation	3 (12.0)	4 (13.0)	–	–

Unless indicated otherwise, data are given as the mean ± SD or n (%). BMI, body mass index; CG, control group; DCM, dilated cardiomyopathy; ECG, electrocardiogram; ILVNC, isolated left ventricular noncompaction; LAX, long-axis view; NC/C, noncompacted to compacted; SAX, short-axis view.

Results

Baseline characteristics

The final analysis was performed on 25 patients with ILVNC and 30 with DCM (*Figure 1*), as well as 30 healthy controls. There were no significant differences in age (P=0.13), gender (P=0.54), or BMI (P=0.25) across the 3 groups. There were significant differences in the NC to C ratio in end-diastole between the ILVNC and DCM groups, both on long- and short-axis views (P<0.001). Chest tightness and shortness of breath were the most common clinical manifestations of ILVNC and DCM. Electrocardiogram abnormalities were common in patients with LVNC and DCM (*Table 1*).

Conventional cardiac function parameters for each of the 3 groups are presented in *Table 2*. The LV cavity in the ILVNC and DCM groups was significantly larger than in the control group (P<0.001), with end-diastolic and end-systolic volume being greater in the DCM than in the ILVNC group (P=0.03 and P=0.04, respectively). LVEF was significantly lower in both the DCM and ILVNC groups than in the control group (P<0.001), and was significantly lower in the DCM than in the ILVNC group (P=0.04).

Reproducibility

In this study, the consistency of measurement between different observers was evaluated using ICC values. ICC values for basal RS, CS, and LS were 0.905, 0.926, and 0.915, respectively; those for RS, CS, and LS in the middle segment were 0.912, 0.927, and 0.936, respectively; and those for apical RS, CS, and LS were 0.915, 0.918, and 0.939, respectively. ICC values for global RS, CS, and LS were 0.925, 0.916, and 0.923, respectively.

Comparisons of LV myocardium strain parameters among the 3 groups

Global, basal, middle, and apical RS, CS, and LS were significantly lower in the ILVNC and DCM groups than in the control group (P<0.001). Basal CS was significantly lower in the DCM than in the ILVNC group (P=0.05), while middle and apical LS was significantly lower in the

Table 2 Comparisons of conventional cardiac function parameters

Variables	ILVNC (n=25)	DCM (n=30)	CG (n=30)	F	P value	LSD (P value)		
						ILVNC *vs*. DCM	ILVNC *vs*. CG	DCM *vs*. CG
EDV (mL)	218.12±53.16	263.23±78.25	125.39±22.51	37.620	<0.001	0.03	<0.001	<0.001
ESV (mL)	171.65±68.23	213.91±73.09	49.94±13.42	56.199	<0.001	0.04	<0.001	<0.001
SV (mL)	64.66±23.22	61.83±35.22	75.46±14.98	1.772	0.18	–	–	–
LVEF (%)	31.63±13.52	24.52±9.32	60.41±6.95	95.349	<0.001	0.04	<0.001	<0.001
CO (%)	5.54±2.70	4.61±2.72	5.53±1.24	1.259	0.29	–	–	–

Unless indicated otherwise, data are given as the mean ± SD. ILVNC, isolated left ventricular myocardial noncompaction; DCM, dilated cardiomyopathy; CG, control group; LSD, least significant difference; EDV, end-diastolic volume; ESV, end-systolic volume; SV, stroke volume; LVEF, left ventricular ejection fraction; CO, cardiac output.

Table 3 Comparisons of strain parameters among the 3 groups

Variables	ILVNC (n=25)	DCM (n=30)	CG (n=30)	F	P value	LSD (P value)		
						ILVNC *vs*. DCM	ILVNC *vs*. CG	DCM *vs*. CG
Basal								
RS (%)	16.13±7.15	13.54±6.44	35.22±9.29	53.631	<0.001	0.34	<0.001	<0.001
CS (%)	–8.76±2.75	–6.87±2.50	–15.88±2.95	48.298	<0.001	0.05	<0.001	<0.001
LS (%)	–4.93±3.66	–4.07±4.56	–10.23±3.31	17.044	<0.001	0.53	<0.001	<0.001
Middle								
RS (%)	8.56±5.12	7.63±2.82	26.17±6.63	96.322	<0.001	0.59	<0.001	<0.001
CS (%)	–7.90±4.25	–7.20±2.37	–17.95±3.13	85.295	<0.001	0.52	<0.001	<0.001
LS (%)	–4.26±1.97	–6.08±2.12	–12.19±2.50	70.380	<0.001	0.02	<0.001	<0.001
Apex								
RS (%)	6.99±4.58	8.43±4.94	25.66±12.90	29.535	<0.001	0.64	<0.001	<0.001
CS (%)	–8.72±4.49	–8.63±2.68	–19.45±4.33	60.526	<0.001	0.91	<0.001	<0.001
LS (%)	–4.89±2.35	–7.10±1.98	–14.53±2.43	104.488	<0.001	0.01	<0.001	<0.001
Global								
RS (%)	9.10±4.68	8.85±3.83	27.58±6.99	88.041	<0.001	0.90	<0.001	<0.001
CS (%)	–8.03±3.94	–7.45±2.38	–17.65±3.11	81.735	<0.001	0.58	<0.001	<0.001
LS (%)	–5.87±2.34	–5.26±2.29	–12.42±2.45	65.305	<0.001	0.46	<0.001	<0.001

Unless indicated otherwise, data are given as the mean ± SD. ILVNC, isolated left ventricular myocardial noncompaction; DCM, dilated cardiomyopathy; CG, control group; LSD, least significant difference; RS, radial strain; CS, circumferential strain; LS, longitudinal strain.

ILVNC than in the DCM group (P=0.02 and P=0.01, respectively; *Table 3*).

ROC curve analysis

The results of evaluations into the diagnostic performance of apical LS, middle LS, basal CS, end-diastolic volume, end-systolic volume, and LVEF in differentiating ILVNC from DCM are shown in *Figure 3* and *Table 4*. Of these parameters, apical LS was the most effective and has area under the curve (AUC) of 0.883 (95% CI: 0.850–0.977; P<0.001), a sensitivity of 88%, and a specificity 83% at

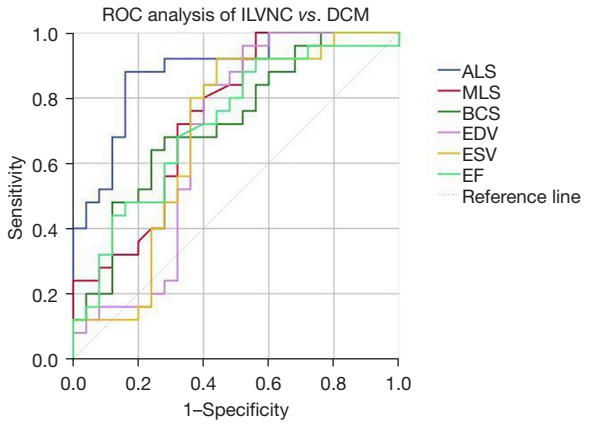

Figure 3 ROC curves of cardiac function and myocardial strain in differentiating ILVNC from DCM. ALS, apex longitudinal strain; BCS, basal circumferential strain; EDV, end-diastolic volume; EF, ejection fraction; ESV, end-systolic volume; MLS, middle longitudinal strain; ROC, receiver operating characteristic; ILVNC, isolated left ventricular myocardial noncompaction; DCM, dilated cardiomyopathy.

a cutoff value of –6.475, as well as the largest positive likelihood ratio for apical LS.

Analysis of the strain pattern in each segment in the 3 groups

From the basal segment to the apex, the RS in the ILVNC and DCM groups was consistent with that in the control group (i.e., basal segment > the middle segment and the middle = the apex, with a decreasing trend). Apical strain of the CS and LS in the DCM and control groups was larger than basal strain, showing a gradually increasing trend; however, no such trend was seen in the ILVNC group, and the LS was more significant (*Table 5*; *Figure 4*).

Discussion

The clinical manifestations of ILVNC lack specificity. LV trabeculations are not a specific manifestation of ILVNC and are often confused with transitional trabeculations caused by DCM (14). The present study provides a method to distinguish these 2 conditions based on functional evaluation (i.e., myocardial strain). In early-stage ILVNC, end-diastolic volume, end-systolic volume, and LVEF could be normal or mildly abnormal, making it easier to distinguish it from DCM. In DCM, excessive trabeculations of the subendocardial myocardium are mostly seen at the end stage of some myocardial diseases and may be accompanied by unexplained LV dilatation, thinning of the ventricle wall, and weakened motion. However, in ILVNC, a cavernous myocardium forms due to the abnormal stagnation of the myocardium compaction process during development. It has been reported that this cavernous myocardium can resist expansion of the myocardium (15).

In late-stage ILVNC, there is significant expansion of the LV and decreased cardiac function, which is similar to DCM with excessive trabeculation of the subendocardium, making it difficult to differentiate the 2 diseases. Myocardial strain parameters can be used to accurately assess the systolic and diastolic function of the myocardium from the circumferential, radial, and longitudinal directions. One study reported that myocardial strain was changed subclinically even in ILVNC patients with normal LVEF (16). In the present study, we also showed that global and segmental RS, CS, and LS in the ILVNC and DCM groups were significantly lower than in the control group. Middle and apical LS were lower in ILVNC than in DCM (P=0.02 and P=0.01, respectively), whereas basal CS was lower in DCM than in ILVNC (P=0.05). The abnormalities in ILVNC are primarily caused by hypertrophy and the disordered myocardial fibers in the NC layer of the subendocardium leading to impaired subendocardial longitudinal myocardial contractility. Therefore, ILVNC primarily affects LS. Our results showed that the global and segmental types of LS were significantly lower in the ILVNC group than in the control group. According to the compaction process of the myocardium, which occurs from the basal segment to the apex and from the epicardium to the endocardium, the apical subendocardium is involved most significantly in most cases of ILVNC, with the basal segment usually not being affected. This explains why middle and apical LS decreased more obviously in ILVNC and was even lower than in DCM, as DCM primarily affects the middle and outer layers of the myocardium; that is, the circumferentially arranged myocardium (17,18), namely CS. In this study, the global and segmental types of CS were significantly lower in the DCM group than in control group. Due to the increase in heart volume and the decrease in systolic function in DCM, compensatory excessive trabeculation of the LV myocardium can occur (primarily in the mid-distal segment) so as to increase the stroke volume by increasing the surface area of the endocardium (19). Therefore, due to the compensatory effect of the mid-distal myocardium, myocardial contractility is not significantly lower than that

Table 4 Cross-tabulation analysis for the index test with the diagnostic standard

Variables	AUC	Sensitivity	Specificity	Accuracy	PPV	NPV	PLR	NLR
ALS	0.883	22/25 (88.0)	25/30 (83.0)	47/55 (85.0)	22/27 (81.0)	25/28 (89.0)	5.280	0.144
MLS	0.745	19/25 (76.0)	18/30 (60.0)	37/55 (67.0)	19/31 (61.0)	18/24 (75.0)	1.900	0.400
BCS	0.723	16/25 (64.0)	23/30 (76.0)	39/55 (71.0)	16/23 (70.0)	23/32 (72.0)	2.743	0.470
EDV	0.680	21/25 (84.0)	18/30 (60.0)	39/55 (71.0)	21/33 (64.0)	18/22 (82.0)	2.100	0.267
ESV	0.686	23/25 (92.0)	17/30 (56.0)	40/55 (73.0)	23/36 (64.0)	17/19 (89.0)	2.123	0.141
LVEF	0.722	17/25 (68.0)	21/30 (70.0)	38/55 (69.0)	17/26 (65.0)	21/29 (72.0)	2.267	0.400

Sensitivity, specificity, accuracy, PPV, and NPV. Data show percentages given in parentheses. AUC, area under the curve; PPV, positive predictive value; NPV, negative predictive value; PLR, positive likelihood ratio; NLR, negative likelihood ratio; ALS, apical longitudinal strain; MLS, midlongitudinal strain; BCS, basal circumferential strain; EDV, end-diastolic volume; ESV, end-systolic volume; LVEF, left ventricular ejection fraction.

Table 5 Comparison of strain parameters in different segments

Variables	Basal	Middle	Apex	F	P value	LSD (P value)		
						Basal *vs*. middle	Basal *vs*. apex	Middle *vs*. apex
ILVNC								
RS (%)	16.13±7.15	8.56±5.12	6.99±4.58	9.483	<0.001	0.002	<0.001	0.49
CS (%)	−8.76±2.75	−7.90±4.25	−8.72±4.49	0.201	0.82	–	–	–
LS (%)	−4.93±3.66	−4.26±1.97	−4.89±2.35	0.239	0.79	–	–	–
DCM								
RS (%)	13.54±6.44	7.63±2.82	8.43±4.94	10.439	<0.001	<0.001	0.001	0.57
CS (%)	−6.87±2.50	−7.20±2.37	−8.63±2.68	3.439	0.04	0.64	0.02	0.05
LS (%)	−4.07±4.56	−6.08±2.12	−7.10±1.98	6.037	0.004	0.03	0.001	0.25
CG								
RS (%)	35.22±9.29	26.17±6.63	25.66±12.90	7.317	0.001	0.002	0.001	0.86
CS (%)	−15.88±2.95	−17.95±3.13	−19.45±4.33	6.446	0.003	0.04	0.001	0.14
LS (%)	−10.23±3.31	−12.19±2.50	−14.53±2.43	15.108	<0.001	0.02	<0.001	0.004

Unless indicated otherwise, data are given as the mean ± SD. LSD, least significant difference; ILVNC, isolated left ventricular myocardial noncompaction; CG, control group; RS, radial strain; CS, circumferential strain; LS, longitudinal strain; DCM, dilated cardiomyopathy.

of the basal segment. This may be why only the basal CS was lower in the DCM than in the ILVNC. group ROC curve analysis in the study showed that of the myocardial strain parameters, apical LS had the highest diagnostic efficacy in distinguishing ILVNC from DCM (AUC 0.883; specificity 88%; sensitivity 83%), which is also because the apex was most significantly involved.

In this study, we also compared strain patterns in different segments between ILVNC and DCM. The results showed that changes in RS in different segments in both groups were consistent with the changes seen in the control group. This is because the essence of active cardiac contraction is the result of the combined force of cardiac CS and LS, whereas the change in RS is the result of the rearrangement of cardiac fibers (20,21). Apical CS and LS were higher than basal CS and LS in the DCM group, which was essentially the same as in the control group but differed from that in the ILVNC group. CS and LS showed a gradual increasing trend from the base to the apex in the control group. This may be related to the morphological

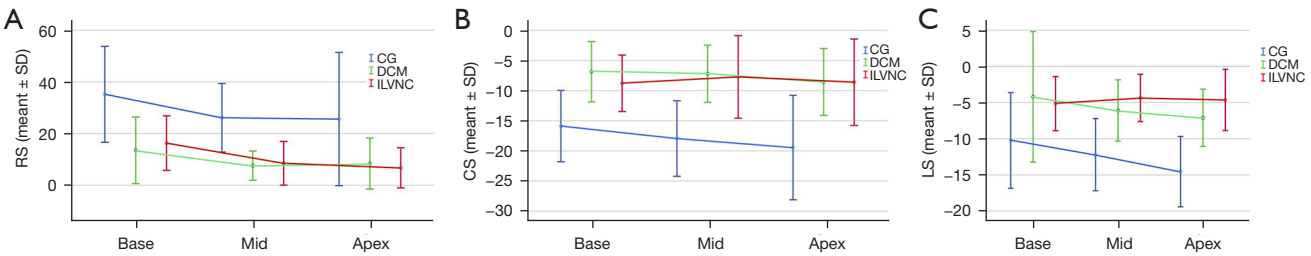

Figure 4 Comparison of changing patterns in (A) RS, (B) CS, and (C) LS in different segments between the control (CG), ILVNC, and DCM groups. (A) Changes in RS from the basal segment to the apex in the ILVNC and DCM groups were consistent with those in the CG group. (B,C) From the basal segment to the apex, the DCM and CG groups showed a gradual upward trend in CS and LS; this change was not seen in the ILVNC group. RS, radial strain; CS, circumferential strain; LS, longitudinal strain; CG, control group; ILVNC, isolated left ventricular myocardial noncompaction; DCM, dilated cardiomyopathy.

characteristics of the heart. The longitudinal and circular muscles meet at the apex. During systole, as the radius of the curvature is gradually reduced from the base to the apex, the apical myocardium has the largest circumferential and longitudinal movement (22). However, there was a large amount of spongy myocardium in the apex of the patients with ILVNC, resulting in weakened motion and decreased strain values in the corresponding parts.

This study has some limitations that should be noted. First, the sample size of the study was small, and the results need to be verified in larger studies. Second, the diagnostic standard in this study was not the gold standard, and there is a possibility of false positives. Third, because ILVNC is a relatively rare disease with a low clinical incidence and because most patients have insignificant early clinical symptoms and a low presentation rate, most LVEF data collected in the ILVNC group in our study showed moderate to severe reductions, and changes in the strain patterns in patients with normal LVEF could not be studied in the different groups.

In conclusion, CMR-FT has considerable potential in the differential diagnosis of ILVNC and DCM when the parameters of global and segmental strain and changes in the pattern of strain from the basal segment to the apex are considered. This is particularly true for patients with ILVNC and significantly reduced LVEF values. CMR-FT can provide more comprehensive and accurate information for clinical differential diagnosis.

Acknowledgments

We would like to thank Kaiyu Wang for her technical support in this study.

Funding: This work was supported by the Shanxi Provincial Health Commission (No. 2020038).

Footnote

Reporting Checklist: The authors have completed the STARD reporting checklist. Available at https://qims.amegroups.com/article/view/10.21037/qims-22-710/rc

Conflicts of Interest: All authors have completed the ICMJE uniform disclosure form (available at https://qims.amegroups.com/article/view/10.21037/qims-22-710/coif). The authors report that this work was supported by the Shanxi Provincial Health Commission (No. 2020038). The authors have no other conflicts of interest to declare.

Ethical Statement: The authors are accountable for all aspects of the work in ensuring that questions related to the accuracy or integrity of any part of the work are appropriately investigated and resolved. This study was conducted in accordance with the Declaration of Helsinki (as revised in 2013) and was approved by the Medical Ethics Committee of Shanxi Cardiovascular Hospital. All participants provided written informed consent.

References

1. Pu C, Hu X, Ye Y, Lv S, Fei J, Albaqali SMAAM, Hu H. Evaluation of myocardial deformation pattern of left ventricular noncompaction by cardiac magnetic resonance tissue tracking. Kardiol Pol 2020;78:71-4.
2. Chen XR, Shu JE, Pan YH, Hu HJ. MRI characteristics of primary dilated cardiomyopathy and isolated left ventricular non-compaction. Chin J Med Imaging Technol 2017; 33:1139-1142.
3. Li XY, Ren WD. Research progresses of left ventricuIar noncompaction. Chin J Med Imaging Technol 2018;34:1716-9.
4. Hussein A, Karimianpour A, Collier P, Krasuski RA. Isolated Noncompaction of the Left Ventricle in Adults. J Am Coll Cardiol 2015;66:578-85.
5. Pryds K, Larsen AH, Hansen MS, Grøndal AYK, Tougaard RS, Hansson NH, Clemmensen TS, Løgstrup BB, Wiggers H, Kim WY, Bøtker HE, Nielsen RR. Myocardial strain assessed by feature tracking cardiac magnetic resonance in patients with a variety of cardiovascular diseases - A comparison with echocardiography. Sci Rep 2019;9:11296.
6. He J, Zhao SH, Lu MJ. Cardiac magnetic resonance feature tracking technique and its progress. Chin J Magn Reson Imaging 2020;11:469-73.
7. Qu YY, Paul J, Li H, Ma GS, Buckert D, Rasche V. Left ventricular myocardial strain quantification with two- and three-dimensional cardiovascular magnetic resonance based tissue tracking. Quant Imaging Med Surg 2021;11:1421-36.
8. Jenni R, Oechslin E, Schneider J, Attenhofer Jost C, Kaufmann PA. Echocardiographic and pathoanatomical characteristics of isolated left ventricular non-compaction: a step towards classification as a distinct cardiomyopathy. Heart 2001;86:666-71.
9. Petersen SE, Selvanayagam JB, Wiesmann F, Robson MD, Francis JM, Anderson RH, Watkins H, Neubauer S. Left ventricular non-compaction: insights from cardiovascular magnetic resonance imaging. J Am Coll Cardiol 2005;46:101-5.
10. Grothoff M, Pachowsky M, Hoffmann J, Posch M, Klaassen S, Lehmkuhl L, Gutberlet M. Value of cardiovascular MR in diagnosing left ventricular non-compaction cardiomyopathy and in discriminating between other cardiomyopathies. Eur Radiol 2012;22:2699-709.
11. Jacquier A, Thuny F, Jop B, Giorgi R, Cohen F, Gaubert JY, Vidal V, Bartoli JM, Habib G, Moulin G. Measurement of trabeculated left ventricular mass using cardiac magnetic resonance imaging in the diagnosis of left ventricular non-compaction. Eur Heart J 2010;31:1098-104.
12. Bozkurt B, Colvin M, Cook J, Cooper LT, Deswal A, Fonarow GC, Francis GS, Lenihan D, Lewis EF, McNamara DM, Pahl E, Vasan RS, Ramasubbu K, Rasmusson K, Towbin JA, Yancy C; American Heart Association Committee on Heart Failure and Transplantation of the Council on Clinical Cardiology; Council on Cardiovascular Disease in the Young; Council on Cardiovascular and Stroke Nursing; Council on Epidemiology and Prevention; and Council on Quality of Care and Outcomes Research. Current Diagnostic and Treatment Strategies for Specific Dilated Cardiomyopathies: A Scientific Statement From the American Heart Association. Circulation 2016;134:e579-646.
13. Chinese Medical Association Cardiovascular Branch, Chinese Myocarditis and Cardiomyopathy Collaborative Group. Chinese guidelines for the diagnosis and treatment of dilated cardiomyopathy. Journal of Clinical Cardiology (China) 2018;34:421-34.
14. Donghi V, Tradi F, Carbone A, Viala M, Gaubert G, Nguyen K, Reant P, Donal E, Eicher JC, Selton-Suty C, Huttin O, Resseguier N, Michel N, Guazzi M, Jacquier A, Habib G. Left-ventricular non-compaction-comparison between different techniques of quantification of trabeculations: Should the diagnostic thresholds be modified? Arch Cardiovasc Dis 2020;113:321-31.
15. Frischknecht BS, Attenhofer Jost CH, Oechslin EN, Seifert B, Hoigné P, Roos M, Jenni R. Validation of noncompaction criteria in dilated cardiomyopathy, and valvular and hypertensive heart disease. J Am Soc Echocardiogr 2005;18:865-72.
16. Liu J, Li Y, Cui Y, Cao Y, Yao S, Zhou X, Wetzl J, Zeng W, Shi H. Quantification of myocardial strain in patients with isolated left ventricular non-compaction and healthy subjects using deformable registration algorithm: comparison with feature tracking. BMC Cardiovasc Disord 2020;20:400.
17. Zhang J, Jiang M, Zheng C, Liu H, Guo Y, Xie X, Zou Z, Zhou X, Xia L, Luo M, Zeng M. Evaluation of isolated left ventricular noncompaction using cardiac magnetic resonance tissue tracking in global, regional and layer-specific strains. Sci Rep 2021;11:7183.
18. Zheng T, Ma X, Li S, Ueda T, Wang Z, Lu A, Zhou W, Zou H, Zhao L, Gong L. Value of Cardiac Magnetic Resonance Fractal Analysis Combined With Myocardial

Strain in Discriminating Isolated Left Ventricular Noncompaction and Dilated Cardiomyopathy. J Magn Reson Imaging 2019;50:153-63.
19. Jiang MC, Zeng M, Guo YY, Xie XZ, Zou ZM, Liu H. MR tissue tracking in assessing isolated left ventricular non-compaction and dilated cardiomyopathy strain. Chin J Med Imaging 2019;27:755-60, 765.
20. Wang H, Yan ZX, Jiang H, Fan ZM, He Y, Dong JZ. Application of cardiac magnetic resonance strain analysis in preclinical apical hypertrophic cardiomyopathy. Chin J Med Imaging 2019;27:1-5.
21. Chen X, Pan J, Shu J, Zhang X, Ye L, Chen L, Hu Y, Yu R. Prognostic value of regional strain by cardiovascular magnetic resonance feature tracking in hypertrophic cardiomyopathy. Quant Imaging Med Surg 2022;12:627-41.
22. Abou R, Leung M, Khidir MJH, Wolterbeek R, Schalij MJ, Ajmone Marsan N, Bax JJ, Delgado V. Influence of Aging on Level and Layer-Specific Left Ventricular Longitudinal Strain in Subjects Without Structural Heart Disease. Am J Cardiol 2017;120:2065-72.

Cite this article as: Zhu L, Wu J, Hao X, Li X. Value of cardiac magnetic resonance feature tracking technology in the differential diagnosis of isolated left ventricular noncompaction and dilated cardiomyopathy. Quant Imaging Med Surg 2023;13(3):1453-1463. doi: 10.21037/qims-22-710

